JOURNAL OF OPTOELECTRONICS AND ADVANCED MATERIALS, Vol. 10, No. 9, September 2008, p. 2298 – 2302

# Designing the colour of photonic crystals for sensors applications

E.VINȚELER[a*], C. FARCĂU[a,b], S. AŞTILEAN[a,b]
[a]*Faculty of Physics, Babeş-Bolyai University, Str. M. Kogalniceanu 1, 400084 Cluj-Napoca, Romania*
[b]*Nanobiophotonics Laboratory, Institute for Interdisciplinar Experimental Research, Babes-Bolyai University, T. Laurian 42, 400271, Cluj-Napoca, Romania*

We present experimental and numerical studies of the color observed from polystyrene colloidal photonic crystals made of 1-4-layers of polystyrene spheres. Simulations allow us to explain the origin of the color we observe under the optical microscope. We show that different colors can be associated unambiguously with different number of layers and type of stacking.

(Received Februry 25, 2008; accepted August 14, 2008)

*Keywords*: Colloidal photonic crystals. Finite-difference time-domain. Sensors

## 1. Introduction

Beautiful iridescent colours in feathers of male peacock, butterfly wings and opal gemstone is the result of nature's clever structural engineering of photonic crystals - three–dimensionally periodic arrays of holes in sponge-like medium (called pepper-pot structure) and of silica spherical units of sub-micron size. Unlike pigments in dyes, which absorb or reflect certain frequencies of light as a result of their chemical composition, photonic crystals reflect light because of their surface characteristics. For example the colours of opal vary with diameter of silica spheres and the alumina coated butterfly wings vary with nanofilm thickness.

The manipulation of optical properties of photonic crystals is of great technological interest [1-2] due to the possibility of producing different colours without the difficulty of synthesising complex pigment molecules. The previous studies have shown that their colour exhibited in transmission and reflectivity depends on a wide range of physical parameters: sphere diameter, refractive index of filling medium, number of layers, stacking pattern etc. These parameters open an attractive way to control the exhibited colour and design novel optical sensors based on the change of colour when photonics crystals are exposed, for example, to humidity, chemical vapour or temperature variation in the environment.

The rather simple and inexpensive way of producing colloidal photonic crystal films made of mono- or multi-layers of dielectric (polystyrene) nano- (micro) spheres received increasing attention because such structures could be used as templates for the creation of metal-dielectric hybrid architectures [3] with plasmonic applications.

In our previous study we analyzed optical properties of monolayer and two-layers of polystyrene spheres [4] and observed that the plate colour changes with the number of layers and diameter of spheres. This motivated us to study the colour of multi-layers with different patterns of packing embedded in media with various indices of refraction. In this article we present experimental and numerical studies of the colour observed from polystyrene colloidal photonic crystals made of 1-4-layers of polystyrene spheres (with refractive index 1.56 and diameter of 400 nm) in hexagonal packing (with lattice step of 400 nm). Three-dimensional finite-difference time-domain (FDTD) simulations allow us to explain the origin of the colour we observe under the optical microscope. We show that different colours can be associated unambiguously with different number of layers and type of stacking.

## 2. Sample fabrication

The colloidal crystal films were fabricated via a convective assembly technique, by using a home-built apparatus [5]. Glass microscope slides of 24x24mm size were used as solid substrates. A droplet of water containing polystyrene spheres (PS) of 400 nm diameter was injected into the wedge between a substrate slide and a deposition slide which is positioned in close proximity with the substrate and tilted by an angle of 27°. As the deposition slide was translated across the substrate, a 2D array of PS self-organized on the substrate due to water evaporation and particles flow from the solution towards the meniscus [6] (see fig. 1).

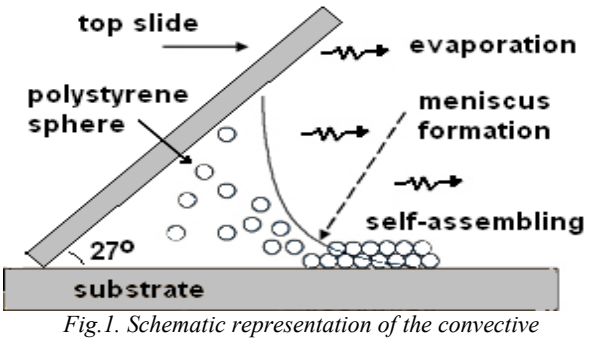


*Fig.1. Schematic representation of the convective assembly technique.*

Diameter of the spheres, concentration of the spheres in solution, speed of the deposition top slide and ambient conditions (humidity and temperature) are the parameters that play on the resulting colloidal film structure [7]. By changing the deposition speed while keeping the rest of the involved experimental parameters unchanged we can control the thickness of the obtained colloidal film.

We inspected the crystallinity of the obtained colloidal films by optical microscopy and scanning electron microscopy (SEM). Optical transmission measurements were performed by using a Jasco V-530 UV-VIS spectrophotometer working with un-polarized light, while for reflectivity we used an interchangeable Jasco SLM-468S reflectivity module on the same apparatus.

## 3. Modeling

Numerical simulations were performed using a finite difference time-domain (FDTD) method [8-10], by means of a freely available software package MEEP (downloadable at MIT site) with subpixel smoothing for increased accuracy [11]. The simulation model propagation of electromagnetic waves using discretized Maxwell's equations in three dimensions taking into account both material shape and dispersion. As shown in Fig. 2, the rectangular computational cell used had dimensions of *a x b x c* grid points, where *a=30, b=52* are the horizontal lattice constants (in grid points - GP) of the hexagonal packing period, and every grid point GP corresponds to 13.33 nm. The vertical size of cell *c* depends on the number of layers and for 4 layers it is 370 grid points. The layers of polystyrene spheres (refractive index n = 1.56) with diameter of 400 nm were placed in the middle of the computational cell, and were surrounded by air on one side, and a half space of glass substrate on the other.

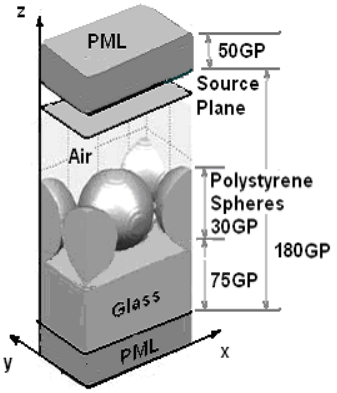


*Fig.2. Schematic representation of the computational cell for one layer of polystyrene spheres.*

A temporally Gaussian pulse was incident normally on the polystyrene spheres layers from the air side. Perfectly matched layer (PML) boundary conditions [12,13] were applied on the boundaries normal to the incident light to prevent reflections (vertical direction), and periodic boundary conditions were applied in the other directions (horizontal directions). The electromagnetic fields at planes located on both sides of the polystyrene spheres layers just before the PMLs were recorded and the Poynting power fluxes were calculated from the discrete Fourier transforms of the fields. This power must be normalized to the incident flux and this implies to repeat the simulation with and without the polystyrene spheres layers. The transmissivity $T^A_{\text{layer}}$ is given by the ratio of the flux through the plane with the layer, over the flux through the same plane, but in the case without the layer. The calculation for the reflectivity $R^A_{\text{layer}}$ is similar, although in this case the incident and reflected fields need to be separated before calculating the flux. The same procedure and calculations must be performed when we calculate $T^G_{\text{layer}}$ and $R^G_{\text{layer}}$. In this case the Gaussian pulse propagates from the glass side.

The transmission through and reflection from the glass substrate alone were calculated using a wave optics formulation. The layers of polystyrene spheres were modeled as sandwiched between two infinite half-spaces of air (n = 1) and glass (n = 1.5), resulting in the transmissivity $T_{\text{layer}}(\omega)$, and reflectivity $R_{\text{layer}}(\omega)$ of the layer alone. On the other side of the glass next to air, Fresnel coefficients were used to calculate the corresponding quantities, $T_{\text{glass}}$=0.96 and $R_{\text{glass}}$=0.04. Ray tracing of the intensity through the glass substrate is then used to calculate the transmission through the entire structure.

The overall transmission and reflection are given by:

$$T_{\text{all}}(\omega) = T^A_{\text{layer}}(\omega) * T_{\text{glass}}/(1 - R_{\text{glass}} * R^A_{\text{layer}}(\omega)),$$
$$R_{\text{all}}(\omega) = R^A_{\text{layer}}(\omega) + T^A_{\text{layer}}(\omega) * T^G_{\text{layer}}(\omega) * R_{\text{glass}}/(1 - R_{\text{glass}} * R^A_{\text{layer}}(\omega)) \quad (1)$$

where we distinguish between the case when incident light is coming first from air (label A) or from glass (label G).

## 4. Results

Conventional optical microscopy allows us to distinguish between colloidal crystal regions of different thickness (different number of layers). We obtained selectively from 1 to 4 layer colloidal films by decreasing the deposition speed from 30 to 9 μm/s at 10% vol colloidal solution concentration.

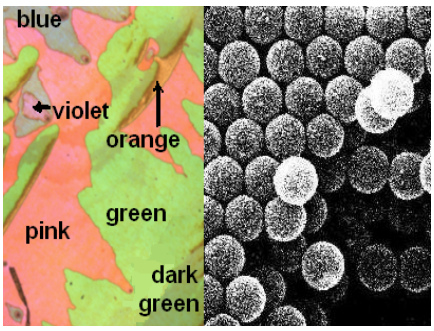


*Fig.3. (left) Optical microscopy image showing areas with different colours corresponding to regions with different number of layers and packing patterns of polystyrene spheres deposited on glass substrate. (right) SEM image showing different number of layers.*

As seen on the left side of fig. 3, under an optical microscope, we have different colored areas for photonic crystals made from colloidal polystyrene spheres deposited on glass substrate. On the right side of fig. 3 the scanning electron microscopy (SEM) image presents a region with different number (at least four) of layers and patterns for hexagonal packing of polystyrene spheres. We expect that these different colored areas match the regions with different number of layers and different patterns: green and darker green for 1 and respectively 2 layers (AB pattern); pink and orange for 3 layers with ABA and, respectively, ABC pattern; blue and violet for 4 layers with ABAB and, respectively, ABCB pattern.

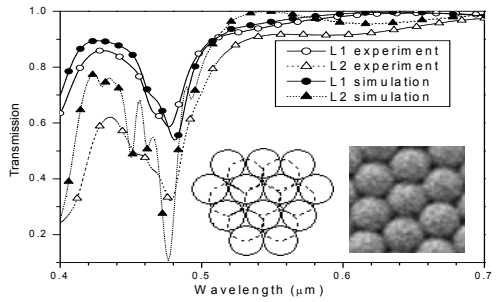


*Fig.4. Measured and simulated transmission spectra of 1 and 2 layers (with AB pattern – see left inset: bottom layer – solid circles, second layer – dotted circles; right inset – SEM image with one layer) of polystyrene spheres with diameter of 400 nm on 1 mm glass substrate.*

In the inset of fig. 4 we see that the spheres self-organized in hexagonal packing in order to minimize the system's energy. The second layer of spheres (dotted circles – B positions) prefer the intermediate positions over first layer spheres (solid circles – A positions) displaying an AB pattern.

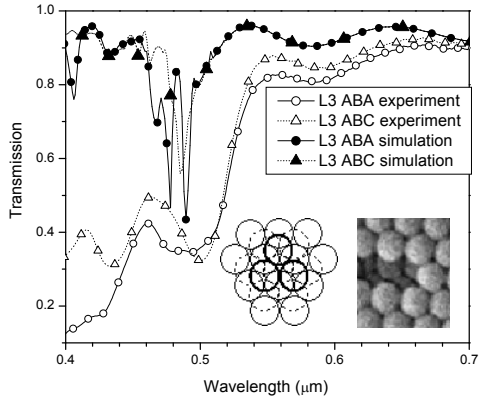


*Fig. 5. Measured and simulated transmission spectra of 3 layers of polystyrene spheres (with 400 nm diameter) with face-centered cub structure (with ABC pattern –see left inset: third layer- thick circles) and hexagonal close-packed structure (with ABA pattern – see left inset: SEM image with two spheres removed) on 1 mm glass substrate*

.

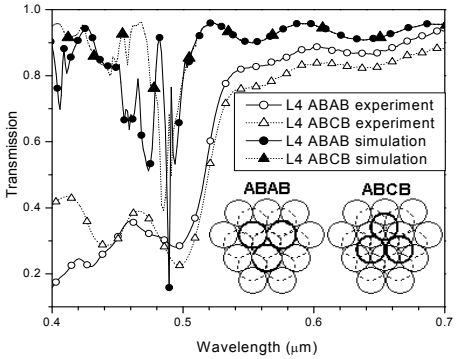


*Fig. 6. Measured and simulated transmission spectra of 4 layers of polystyrene spheres (with 400 nm diameter) with face-centered cub structure (with ABCB pattern – see right inset: fourth layer coincides with second layer – dotted circles) and hexagonal close-packed structure (with ABAB pattern– see left inset: fourth layer coincides with second layer – dotted circles) on 1 mm glass substrate.*

We have observed the very rare AA pattern when second layer spheres stack exactly in the same A positions on the top of first layer spheres, but only on modest scales of order of several spheres. When we add the third layer spheres (represented by thick circles in the inset of fig. 5) we have two choices: ABA or ABC pattern. The fourth layer spheres occupy the same B positions as the second layer spheres (represented by doted circles in the inset of fig. 6).

To prove the hypothesis that different number of layers and different patterns of polystyrene spheres give us different colours, the transmission and reflection at normal incidence of every colored area of the sample have been measured using a spectrometer attached to an optical microscope. The recorded experimental spectra (wavelength range from 0.4 μm to 0.7 μm) for each area of the sample are represented by curves with white circles and triangles in Figs. 4-6 as functions of wavelength. For wavelengths above 0.55 μm, the spectra are quite similar for the same number of layers. For wavelengths below 0.55 μm, the transmission spectra differ and explain the different colors of the samples.

For correct identification of number of layers and structure pattern we simulated in fig. 4-6 the transmission spectra (curves with black circles and triangles). In fig. 4 the transmission spectrum for 1 layer has one minimum at 480 nm giving reflected green colour and the transmission spectrum for 2 layers has two minima at 476 nm and 450 nm giving darker green colour. In Fig. 5 the transmission spectrum for 3 layers with ABA pattern has two minima at 490 nm and 477 nm giving pink colour; for ABC pattern there is one minimum at 486 giving orange colour. In Fig. 6 the transmission spectrum for 4 layers with ABAB pattern has again two minima: one at 490 nm and at 475 nm giving blue colour; for ABCB pattern there are two minima at 490 nm and 483 nm giving violet colour.

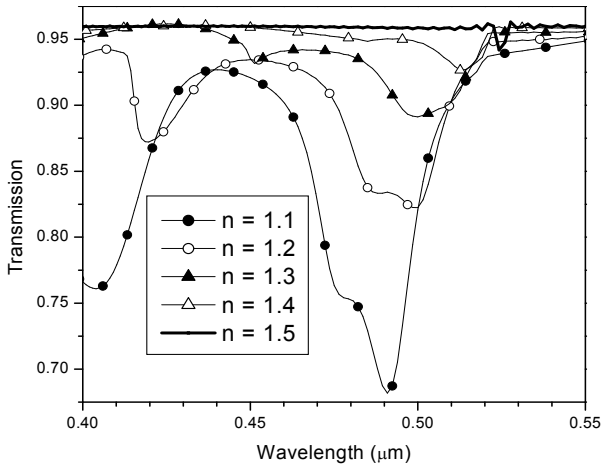


*Fig. 7. Simulated transmission spectra for a monolayer of polystyrene spheres embedded in media with refractive indices ranging from n=1.1 to 1.5.*

We are further investigating the dependence of the optical properties of colloidal crystal films on changes of the environment's refractive index. In Fig. 7 we can see that by varying the medium refractive indices from 1.1 to 1.5, the bandgap of a monolayer of polystyrene spheres shifts from 490 nm to 525 nm and the associated reflected colour changes from green to pink. This will allow us to design novel optical sensors based on the change of colour when photonic crystals are exposed, for example, to humidity, chemical vapour or temperature variation in the environment.

## 5. Discussion

When we compare theory with experiment (see fig. 4-6) we observe two differences:

The experimental transmission falls slowly when we pass from high to low wavelengths due to absorption in glass substrate (significant for wavelengths under 0.46 μm). The simulation does not take in account this absorption and the theoretical transmission is on average at the same level.

We observe that the experimental transmission spectra are smeared at dips compared to simulations and we have the following explanations: In experiment the light is transmitted through a square region containing 5000x5000 polystyrene spheres and, unfortunately this is not a perfect photonic crystal (as it is in simulations). We have a network of tree-like defects - a usual picture in real crystals - that modifies transmittance.

Sometimes the smeared experimental dip can hidden several close-positioned dips as can be seen in fig.5 for wavelength range 0.47-.51 μm when we compare experimental curve (white circles) with simulation curve (black circles) for ABA pattern. Simulation suggests we have three near minima instead of a smeared dip. The same is true for four layers with ABAB pattern as can be seen in fig.6 for the same wavelength range 0.47-.51 μm when we compare experiment with simulation. .

Because we do not use absorption and frequency-dependent refractive indices in simulation, our model is scale independent and can be compared with other simulations for polystyrene spheres with different diameters. Our results for four layers are in good agreement with those of the work [14] in which were measured and simulated polystyrene spheres with refractive index 1.57 and diameter 870 nm on glass substrate with refractive index 1.45. In work [14] was studied also ABCA pattern, but unfortunately we did not find on our slab a large region with ABCA pattern to measure transmittance.

## 6. Conclusions

We have shown, both theoretically and by experiment that the colour of colloidal photonic crystal films exhibited in transmission and reflectivity depends on the number of layers, stacking pattern and environment's refractive index. We found good agreement between theoretical spectra obtained by three-dimensional finite-difference time-domain (FDTD) simulations and measured spectra. By these means we can explain the origin of the color observed under the optical microscope and distinguish unambiguously areas with different number of layers or type of stacking.

**Acknowledgments**

This research was supported by the Romanian Agency for Scientific Research under the project CEEX 71/2006 (Matnantech).

## References

[1] K. Sakoda, Optical properties of photonic crystals, Springer, (2001)
[2] E. Pavarini, L.C. Andreani, C. Soci, M. Galli, F. Marabelli, D. Comoretto, Phys. Rev. B, **72**, 045102 (2005).
[3] C. Farcău, S. Aştilean, J. Opt. A: Pure Appl. Opt., **9**, S345 (2007).
[4] C. Farcău, E.Vinţeler, S. Aştilean, Experimental and Theoretical Investigation of Optical Properties of Colloidal Photonic Crystal Films, submitted to J. Optoelectron. Adv..Mater.
[5] A. Kuttesch, C. Farcău, Z. Neda, S. Aştilean, Proc. SPIE, **6785**, 678500 (2007).
[6] P.A. Kralchevsky, N.D. Denkov, Current opinion in colloid & interface Sci, **6**, 383 (2001)
[7] B.G.Prevo, O.D.Velev, Langmuir, **20**, 2099 (2004)
[8] A. Taflove and S. C. Hagness, Computational Electrodynamics: The Finite-Difference Time-Domain Method, 3rd ed. Artech House, Norwood, MA, (2000).
[9] J. D. Joannopoulos, R. D. Meade, and J. N. Winn, Photonic Crystals, Princeton University Press, Princeton, NJ, (1995).
[10] S. G. Johnson and J. D. Joannopoulos, Photonic Crystals: The Road from Theory to Practice, Kluwer,

Boston, (2002).
[11] A. Farjadpour, D. Roundy, A. Rodriguez, M. Ibanescu, P. Bermel, J. D. Joannopoulos, S.G. Johnson, G. Burr, Optics Letters **31**, 2972 (2006).
[12] P. Lalanne and E. Silberstein, Opt. Lett. **25**, 1092 (2000).
[13] E. Silberstein, P. Lalanne, J.-P. Hugonin, and Q. Cao, J. Opt. Soc. Am. A **18**, 2865 (2001).
[14] X. Checoury, S. Enoch, C. López and A. Blanco, App. Phys. Lett. **90**, 161131 (2007).

*Corresponding author: evinteler@phys.ubbcluj.ro